# Osmotic virial coefficients for model protein and colloidal solutions: Importance of ensemble constraints in the analysis of light scattering data

**4 AUTHORS**, INCLUDING:

Daniel W Siderius

National Institute of Standards and Technolo…

**30** PUBLICATIONS   **159** CITATIONS

SEE PROFILE

# Osmotic virial coefficients for model protein and colloidal solutions: Importance of ensemble constraints in the analysis of light scattering data

Daniel W. Siderius, William P. Krekelberg, Christopher J. Roberts, and Vincent K. Shen
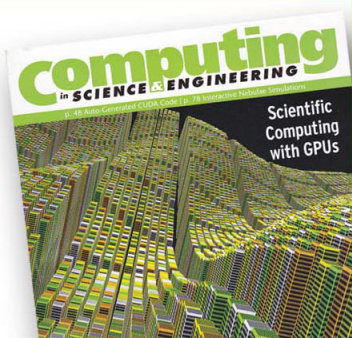
# Osmotic virial coefficients for model protein and colloidal solutions: Importance of ensemble constraints in the analysis of light scattering data

Daniel W. Siderius,[1,a)] William P. Krekelberg,[1] Christopher J. Roberts,[2,3] and Vincent K. Shen[1]

[1]*Chemical and Biochemical Reference Data Division, National Institute of Standards and Technology, Gaithersburg, Maryland 20899, USA*
[2]*Department of Chemical Engineering and Center for Molecular and Engineering Thermodynamics, University of Delaware, Newark, Delaware 19716, USA*
[3]*NIST Center for Neutron Research, National Institute of Standards and Technology, Gaithersburg, Maryland 20899, USA*

Protein-protein interactions in solution may be quantified by the osmotic second virial coefficient (OSVC), which can be measured by various experimental techniques including light scattering. Analysis of Rayleigh light scattering measurements from such experiments requires identification of a scattering volume and the thermodynamic constraints imposed on that volume, i.e., the statistical mechanical ensemble in which light scattering occurs. Depending on the set of constraints imposed on the scattering volume, one can obtain either an apparent OSVC, $A_{2,app}$, or the true thermodynamic OSVC, $B_{22}^{osm}$, that is rigorously defined in solution theory [M. A. Blanco, E. Sahin, Y. Li, and C. J. Roberts, J. Chem. Phys. **134**, 225103 (2011)]. However, it is unclear to what extent $A_{2,app}$ and $B_{22}^{osm}$ differ, which may have implications on the physical interpretation of OSVC measurements from light scattering experiments. In this paper, we use the multicomponent hard-sphere model and a well-known equation of state to directly compare $A_{2,app}$ and $B_{22}^{osm}$. Our results from the hard-sphere equation of state indicate that $A_{2,app}$ underestimates $B_{22}^{osm}$, but in a systematic manner that may be explained using fundamental thermodynamic expressions for the two OSVCs. The difference between $A_{2,app}$ and $B_{22}^{osm}$ may be quantitatively significant, but may also be obscured in experimental application by statistical uncertainty or non-steric interactions. Consequently, the two OSVCs that arise in the analysis of light scattering measurements do formally differ, but in a manner that may not be detectable in actual application. © *2012 American Institute of Physics.*
[http://dx.doi.org/10.1063/1.4709613]

## I. INTRODUCTION

In protein biophysics and colloid science, the osmotic second virial coefficient (OSVC) is often used to quantify interactions between species in solution, in particular protein-protein interactions.[1–5] The OSVC is rigorously defined from thermodynamics (see Sec. II A) and may be measured experimentally using laboratory techniques including laser light scattering,[6–9] sedimentation equilibrium,[10–14] classical osmometry,[15, 16] and others.[17–23] From statistical mechanics, the OSVC, denoted here as $B_{22}^{osm}$, may be related to an integral of the protein-protein potential of mean force in the limit of low protein concentration (e.g., Eq. (6)),[1,2] analogous to usual virial coefficients that are related to pair potential functions. We note, however, that the correct OSVC is only obtained when the potential of mean force is computed in a grand canonical ensemble; otherwise the computed term has a different thermodynamic meaning.[1,2]

Beyond its strict statistical mechanical interpretation, the OSVC serves as an important qualitative and quantitative indicator of protein-protein interactions and is useful for understanding protein behaviors such as crystallization,[3, 24–27] fluid-phase equilibria,[28–30] aggregation,[4, 22, 31–34] and purification[35–37] that may be technologically exploited. Qualitatively, the sign and relative magnitude of $B_{22}^{osm}$ are thought to be indicative of the nature of the net protein-protein interactions.[2, 34, 38–42] For example, if we define $B_{22}^{hs}$ as the equivalent hard-sphere (HS) second virial coefficient, then $B_{22}^{osm}/B_{22}^{hs} > 1$ is interpreted to mean that the interaction is dominated by non-steric repulsion between protein molecules. Conversely, $B_{22}^{osm}/B_{22}^{hs} < 1$ is thought to indicate that attractions between protein molecules dominate the interaction.

In a recent paper by one of the present authors,[43] the connections between light scattering physics, thermodynamics, and statistical mechanics were reexamined and the results therein proposed a revised analysis of scattering measurements from an otherwise standard laser light scattering experiment. As in the traditional analysis of light scattering, the revised analysis relates the average scattered intensity to thermodynamic quantities such as the OSVC and an apparent molecular weight. In the traditional formulation of light scattering analysis by Stockmayer (see Sec. II B for additional details), Rayleigh scattering for a solution of protein, solvent,

---
a)Author to whom correspondence should be addressed. Electronic mail: daniel.siderius@nist.gov.

and some number of cosolvents may be written as[6]

$$\frac{R_{90}^{ex}}{K'(\xi_2)^2} = \frac{c_2(M_{2,app}/M_2)}{1 + 2c_2 A_{2,app}}, \tag{1}$$

in which $R_{90}^{ex}$ is the excess scattering ratio (measured at 90° relative to the incident beam), $K' = 4\pi^2 n^2/\lambda^2$ ($n$ is the refractive index and $\lambda$ is the incident beam wavelength), $\xi_2$ is a physical property that will be defined later, $c_2$ is the protein concentration (in molar or number units), $M_2$ and $M_{2,app}$ are the true and apparent molecular weights, respectively, and $A_{2,app}$ is a term similar to the OSVC. [The terms in Eq. (1) are often given in mass units since $M_2$ is usually not known *a priori*, so that $c_2$ and $1/A_{2,app}$ have units of mass/volume. In this paper, we use molar units to avoid explicit introduction of a molecular weight. Equation (1) can be converted to mass units by multiplying both sides by $(M_2)^2$.] Equation (1) is derived by assuming that the scattering volume is at fixed pressure and contains a fixed number of solvent molecules (typically water), but is open to exchange of protein and any other species. (Additionally, all species are assumed to be nondissociable, though this can be at least approximately considered by accounting for Donnan equilibria.[44]) Since $A_{2,app}$ is defined at fixed pressure ($p$) and fixed number of solvent molecules ($N_1$), $A_{2,app}$ may be expected to differ from $B_{22}^{osm}$, which is defined in a grand canonical ensemble (see discussion in Sec. II A). In contrast to the traditional analysis of light scattering in which pressure and $N_1$ are fixed, Blanco *et al.* formulated the analysis of light scattering for a fixed scattering volume open to exchange of all species (a grand canonical ensemble), which yielded[43]

$$\frac{R_{90}^{ex}}{K'(\eta_2)^2} = \left(\frac{M_{2,app}}{M_2}\right) c_2 - 2B_{22}^{osm} c_2^2, \tag{2}$$

in which $\eta_2$ is a physical property that will be defined later and all other terms are as defined previously. (We note that Eqs. (1) and (2) both contain an apparent molecular weight but that the respective definitions of $M_{2,app}$ are not formally identical.[43]) In Eq. (2), the OSVC is not a surrogate like $A_{2,app}$ but is the true $B_{22}^{osm}$. Blanco *et al.* argued that Eq. (2) is the correct mathematical relationship between the scattered light ratio and properties of the protein species, since the most natural scattering volume is one of fixed volume that is able to exchange all molecular components with the surrounding fluid.[43]

Equation (2) may be rewritten in a form resembling Stockmayer's equation (1) to yield a term similar to $A_{2,app}$, but that resultant term is only equivalent to $B_{22}^{osm}$ when the protein is at near-infinite dilution and if Donnan effects can be neglected (see Eqs. (27) and (28) of Ref. 43 and associated discussion). Doing so does, however, require one to relax the assumptions of constant $p$ and $N_1$ that are implicit in many treatments.[6,13,14,34,44] On general thermodynamic grounds, one may expect differences between a system held at fixed ($T, V, \mu_1, \mu_2, \mu_3, \ldots$) and one held at fixed ($T, p, N_1, \mu_2, \mu_3, \ldots$). From a quantitative perspective, however, it is not clear whether the differences would be significant for an aqueous protein solution. It is therefore desirable to examine and compare $B_{22}^{osm}$ and $A_{2,app}$ to more clearly understand how they differ. As a first step, we investigate how these two

quantities differ in a simple fluid model, namely the multi-component HS fluid. The HS fluid is an important reference state for discussing osmotic effects in protein and colloidal solutions[45–53] and has been recently applied to the interpretation of light scattering data.[54] Here we utilize the Boublik-Mansoori-Carnahan-Starling-Leland (BMCSL) equation of state (EOS) for HS mixtures[55–57] to obtain the thermodynamic quantities necessary to compute $B_{22}^{osm}$ and $A_{2,app}$ for various solution conditions (pressure or volume fraction, cosolvent molality, and size of solution species). Because the two OSVCs are calculated using the same EOS, they can be compared unambiguously and, as we show, provide guidance concerning the relationship between $A_{2,app}$ and $B_{22}^{osm}$. Lastly, a clear understanding of the difference or lack thereof between $A_{2,app}$ and $B_{22}^{osm}$ for a simple model may prove useful when comparing experimental data to computed values (e.g., from molecular simulation) or while determining if other effects (e.g., Donnan contributions or monomer-oligomer equilibria) are important.

This paper is organized as follows. In Sec. II we review the thermodynamic derivation of the proper OSVC, $B_{22}^{osm}$, the light scattering physics relationships that lead to Eqs. (1) and (2), and essential details of the BMCSL EOS. Section III describes our method for computing $B_{22}^{osm}$ and $A_{2,app}$ from the BMCSL EOS. We compare the computed values of $B_{22}^{osm}$ and $A_{2,app}$, for both a binary solution (solvent and protein) and ternary solutions (solvent, protein, and cosolvent) in Sec. IV. The implications of our results are discussed in Sec. V. Our results and key conclusions are summarized in Sec. VI.

## II. BACKGROUND

Before discussing our calculations of various "osmotic second virial coefficients" as defined in different ensembles, it is valuable to review the basic definition of these various OSVCs and discuss their relationship to light scattering physics. We will also provide a brief review of the HS thermodynamic model used for calculations in Sec. IV. The discussion that follows draws from both statistical mechanics and macroscopic thermodynamics, but all calculations and resultant conclusions will be taken in the macroscopic limit where system size effects are negligible.

### A. The osmotic second virial coefficient

We begin by reviewing the derivation of the OSVC, based on the McMillan-Mayer Theory of Solutions[58] as presented in a more accessible form by Ben-Naim.[2] For our discussion, we adopt Scatchard's notation[59] for identification of the constituent species in a protein solution, in which the solution is composed of a solvent species (labeled 1), a protein species (labeled 2), and some number of cosolvent or other solute species (labeled 3, 4, etc.). We restrict our discussion to a single cosolvent species, but the concept can be straightforwardly extended to a solution with multiple cosolvents. In a classic membrane osmometry experiment, the solution might be composed of water (1), protein (2), and some cosolvent (3) such as a salt or urea, where the protein cannot pass through the membrane.

The OSVC is defined via a virial expansion of the osmotic pressure of a solution as a function of the concentration (density) of protein,

$$\frac{\Pi(T, \mu_1, c_2, \mu_3)}{kT} = c_2 + B_{22}^{osm}(T, \mu_1, \mu_3)\, c_2^2 + \cdots, \quad (3)$$

where $\Pi$ is the osmotic pressure, $c_2 = N_2/V$ is the protein concentration ($N_i$ is number of molecules of species $i$ and $V$ is the volume of the solution containing protein), $k$ is Boltzmann's constant, $T$ is the solution temperature, and $\mu_i$ is the chemical potential of species $i$. As noted, $\Pi$ is measured at fixed temperature and chemical potential of solvent and co-solvent. Application of the Gibbs-Duhem relation to Eq. (3) yields one definition of the OSVC,

$$B_{22}^{osm} = \frac{1}{2} \lim_{c_2 \to 0} \left[ \frac{V}{kT} \left( \frac{\partial \mu_2}{\partial N_2} \right)_{T,V,\mu_{k\neq2}} - \frac{V}{N_2} \right]. \quad (4)$$

If we instead appeal to statistical mechanics, the osmotic pressure may be written as

$$\Pi(T, V, \mu_1, \mu_2^*, \mu_3,) = kT \ln \left[ \frac{\Xi(T, V, \mu_1, \mu_2^*, \mu_3)}{\Xi(T, V, \mu_1, \mu_3)} \right], \quad (5)$$

where $\Xi(T, V, \mu_1, \ldots, \mu_m)$ is the grand canonical partition function for an $m$-species system at fixed $T$, $V$, and chemical potentials ($\mu_i$) of all species. $\mu_2^*$ is the chemical potential of species 2 that yields the desired $c_2 = N_2/V$, as computed in the grand canonical ensemble. After extensive manipulation,[2,58] Eqs. (3) and (5) yield

$$B_{22}^{osm} = -\frac{1}{2} \int \left\{ \exp\left[ -W_{22}^{(0)}(r)/kT \right] - 1 \right\} 4\pi r^2 dr, \quad (6)$$

where $W_{22}$ is the protein-protein potential of mean force (averaged over all spatial degrees of freedom) and the superscript (0) indicates that it is taken in the infinitely dilute limit, e.g., $c_2 \to 0$ or $\mu_2 \to -\infty$. In this form, the OSVC is analogous to the usual pressure virial coefficient (i.e., for a dilute gas) with the replacement of the pair potential by $W_{22}$. Equivalently,[2,58]

$$B_{22}^{osm} = -\frac{1}{2} \int \left[ \bar{g}_{22}^{(0)}(r) - 1 \right] 4\pi r^2 dr, \quad (7)$$

where $\bar{g}_{22}^{(0)}$ is the pair distribution function of species 2, taken in the infinitely dilute limit and the overbar indicates that it is computed in the grand canonical ensemble. Equation (7) may also be rewritten as

$$\begin{aligned} B_{22}^{osm} &= -\frac{1}{2} \lim_{c_2 \to 0} G_{22} \\ &= -\frac{1}{2} \lim_{c_2 \to 0} \left[ V \frac{kT}{(N_2)^2} \left( \frac{\partial N_2}{\partial \mu_2} \right)_{T,V,\mu_{k\neq2}} - \frac{V}{N_2} \right], \end{aligned} \quad (8)$$

in which $G_{ij}$ is the $i$-$j$ Kirkwood-Buff integral.[1] Equations (4) and (8) yield the same $B_{22}^{osm}$, but only in the specified dilute limit.

## B. Light scattering and thermodynamics

Laser light scattering is a useful analytical tool since scattering measurements may be exploited to yield thermody-namic properties that quantify intermolecular interactions. In the theory of Einstein, the Rayleigh scattering ratio from point scatterers (small in size relative to incident beam wavelength) measured at $90°$ relative to the incident beam is related to the ensemble-averaged fluctuation in refractive index according to

$$R_{90} = \frac{4\pi^2 n^2 \langle (\Delta n)^2 \rangle V}{\lambda^4}, \quad (9)$$

in which $V$ is the scattering volume and $\lambda$ and $n$ are as defined previously. The $\langle \cdots \rangle$ brackets indicate an ensemble average, though the constraints that define that ensemble have not yet been specified. In many classic treatments of laser light scattering,[6,60] $\langle (\Delta n)^2 \rangle$ is related to fluctuations in the number of molecules (moles) of each constituent species in the scattering volume in the selected ensemble, and further to derivatives of the number of molecules with respect to chemical potential. For a detailed discussion of the derivations that transform Eq. (9) into a more experimentally useful form, see Ref. 43.

To date, most applications of laser light scattering to analyze protein-protein interactions are based, at least in part, on the approximations introduced by Stockmayer (i.e., constant $N_1$ and pressure for the scattering control volume).[6] In his treatment of light scattering, fluctuations in the refractive index were taken in a scattering volume at fixed $T$, pressure, $N_1$, and chemical potential of the solute and cosolvent species ($\mu_2$ and $\mu_3$). With these constraints defining the ensemble, the fluctuation in the refractive index may be written as[43]

$$\begin{aligned} \langle \Delta n^2 \rangle &= kT \sum_{i=2}^{C} \sum_{j=2}^{C} \xi_i \xi_j \left( \frac{\partial N_i}{\partial \mu_j} \right)_{T,p,N_1,\mu_{k\neq j}} \\ &- \frac{kT}{\kappa_T V} \left[ \left( \frac{\partial n}{\partial p} \right)_{T,\mathbf{N}} \right]^2, \end{aligned} \quad (10)$$

in which $\xi_i = V \cdot (\partial n/\partial N_i)_{T,p,N_{k\neq i}}$ (essentially the response of the refractive index to a change in concentration of species $i$), $\kappa_T$ is the isothermal compressibility, and all other terms are as previously defined. (We note that $V$ is an ensemble-average quantity that must fluctuate, since scattering is assumed to occur in a fixed pressure scattering volume.) Introduction of the above equation into Eq. (9), transformation of the derivatives while assuming no coupling between the concentrations of protein and cosolvent, and significant algebraic manipulation yields Eq. (1), which gives the excess scattering ratio at low concentration of species 2 ($N_2 \to 0$).[6,43] $A_{2,app}$ may be expressed in a number of equivalent forms, including one similar to that of Stockmayer,[6]

$$\begin{aligned} A_{2,app} = \frac{1}{2} \lim_{N_2 \to 0} \Bigg\{ &\frac{V}{kT} \Bigg[ \left( \frac{\partial \mu_2}{\partial N_2} \right)_{T,p,N_1,N_3} \\ &- \frac{[(\partial \mu_2/\partial N_3)_{T,p,N_1,N_2}]^2}{(\partial \mu_3/\partial N_3)_{T,p,N_1,N_2}} \Bigg] - \frac{V}{N_2} \Bigg\}, \end{aligned} \quad (11)$$

which is convenient for experimental application since the derivatives of $\mu_i$ are at fixed $T$, $p$, and $N_i$ and may be converted to derivatives of activity coefficients with respect to molality.

One can also write

$$A_{2,app} = \frac{1}{2} \lim_{N_2 \to 0} \left[ \frac{V}{kT} \left( \frac{\partial \mu_2}{\partial N_2} \right)_{T,p,N_1,\mu_3} - \frac{V}{N_2} \right], \quad (12)$$

which is similar to Eq. (4), though with the change to a derivative at constant $p$ and $N_1$ and the necessity of defining the volume through an ensemble average. Lastly, our preferred form for the present report is[43]

$$A_{2,app} = -\frac{1}{2} \lim_{c_2 \to 0} \left[ G_{22} + \left( \frac{V}{N_1} + G_{11} - 2G_{12} \right) \right]. \quad (13)$$

In Eq. (13), the $G_{ij}$ Kirkwood-Buff integrals are defined in the grand canonical ensemble, not the isothermal-isobaric semigrand ensemble used by Stockmayer. We prefer this expression of $A_{2,app}$ for reasons of compactness and ease of comparison with $B_{22}^{osm}$. $A_{2,app}$ is termed the "apparent OSVC" of species 2, but is not formally equivalent to either of Eq. (4) or Eq. (8). However, the terms other than $G_{22}$ in the brackets in Eq. (13) may not be large or may compensate for one another in practical examples. A major objective of this work is to determine if those terms may be safely neglected, using the calculations and model systems described below.

As mentioned previously, Blanco *et al.* reconsidered the classic treatment of light scattering by rederiving the thermodynamic relationships for a scattering system that is fixed in volume and open to the exchange of all molecular species. With these constraints, the fluctuation in the refractive index is given by

$$\langle \Delta n^2 \rangle = kT \sum_{i=1}^{C} \sum_{j=1}^{C} \eta_i \eta_j \left( \frac{\partial N_i}{\partial \mu_j} \right)_{T,V,\mu_{k \neq j}}, \quad (14)$$

in which $\eta_i = V \cdot (\partial n / \partial N_i)_{T,V,N_{k \neq i}}$. Use of the above equation in Eq. (9) in the limit of low protein concentration yields the scattering relation in Eq. (2). (For finite protein concentration, $B_{22}^{osm}$ is replaced by $-G_{22}/2$, see Ref. 43.) In Eq. (2), the $B_{22}^{osm}$ term is exactly that given in Eq. (8) and, as such, is the true OSVC of species 2 when scattering is performed at sufficiently low $c_2$.

## C. BMCSL equation of state for hard-sphere mixtures

All calculations in this paper will utilize the BMCSL EOS (Refs. 55–57) for mixtures of hard spheres. The BMCSL EOS is the multicomponent analog of the Carnahan-Starling EOS (Ref. 61) for a single component HS fluid. It only requires as input the diameters of each HS component in the fluid ($\sigma_i$), the component mole fractions ($x_i$), and either the total density or volume fraction ($N/V$ or $\phi$), from which it returns all of the thermodynamic properties necessary for our calculations. The BMCSL EOS is derived in the thermodynamic limit where system size does not affect intensive properties. Consequently, our use of this EOS implicitly invokes the equivalence of statistical mechanical ensembles and the resultant equality of non-fluctuation properties in different ensembles (e.g., $\langle N_i \rangle \to N_i$, etc.). Since the natural independent variables of the EOS correspond to the canonical ensemble, some manipulation is required to compute thermodynamic derivatives and fluctuation quantities in either

the grand canonical ensemble or Stockmayer's isothermal-isobaric semigrand ensemble.

## III. CALCULATION METHODS

$B_{22}^{osm}$ has been obtained analytically from the BMCSL EOS for a binary HS fluid containing a solute and solvent by Simonin[47] but, to our knowledge, not for solutions containing more than two components. General analytic solutions for $B_{22}^{osm}$ and $A_{2,app}$ are not yet available from the EOS, and may not be possible, so we compute them numerically using the following procedure.

For calculations taken at a specified volume fraction ($\phi = \sum_i \pi N_i \sigma_i^3 / 6V$):

1. Set the molality of the cosolvent species ($m_3 = N_3/N_1$) and the HS diameters relative to species 1 ($\sigma_2/\sigma_1$ and $\sigma_3/\sigma_1$).
2. Choose a large $V$ to avoid numerical artifacts from small $N_i$. (We used $V/\sigma_1^3 = 10^5$. Intensive properties from the BMCSL EOS do not depend on $V$, but small $N_i$ can lead to issues with numerical precision.)
3. Select a starting guess of the mole fraction of species 2, $x_2$. (We used $x_2 = 10^{-4}$.)
4. From $x_2$ and $m_3$, compute the entire composition vector **x**.
5. Given $V$, $\phi$, and **x**, compute **N**.
6. Compute all $G_{ij}$ and, thereby, $B_{22}^{osm}$ and $A_{2,app}$.
7. If $B_{22}^{osm}$ and $A_{2,app}$ have converged to specified tolerance, output answers, otherwise, reduce $x_2$ and repeat from step 4.

(We note that, in the BMCSL EOS, $N_i$ are not necessarily integer quantities.) In all cases, $B_{22}^{osm}$ and $A_{2,app}$ were computed subject to a relative tolerance of $10^{-6}$ or smaller. When our method is applied to a single-component HS solvent, the numerical results for $B_{22}^{osm}$ match the analytic result of Simonin.[47] To compute $B_{22}^{osm}$ and $A_{2,app}$ for a specified $p$, we modify the procedure slightly: For a given composition and following step 4, we add a step in which we iteratively compute the $\phi$ that gives the desired $p$ for the specified $V$ and **x**. The procedure is otherwise identical. Our method for computing OSVCs may be straightforwardly extended to HS mixtures of more than three components.

Kirkwood-Buff $G_{ij}$ integrals were computed from derivatives of $\mu_i$ taken in the canonical ensemble using a standard algebraic manipulation.[1] First, one defines

$$A_{ij} = \left( \frac{\partial \mu_i}{\partial N_j} \right)_{T,V,N_{k \neq j}} = A_{ji}, \quad (15)$$

and **A** is defined as the matrix containing elements $A_{ij}$. Then, utilizing equivalence of ensembles and a Jacobian transformation,

$$G_{ij} = \frac{V}{N_i} \left[ \frac{kT}{N_j} \left( \frac{\partial N_i}{\partial \mu_j} \right)_{T,V,\mu_{k \neq j}} - \delta_{ij} \right]$$

$$= \frac{V}{N_i} \left[ \frac{kT}{N_j} \frac{A^{ij}}{|\mathbf{A}|} - \delta_{ij} \right]. \quad (16)$$

$A^{ij}$ is the cofactor of element $A_{ij}$ in **A** and $\delta_{ij}$ is the Kronecker delta. $A_{ij}$ are obtained analytically from the BMCSL EOS.

## IV. RESULTS

In this section, we compare $B_{22}^{osm}$ and $A_{2,app}$ calculated using the BMCSL EOS for HS solutions. All results are presented using normal HS reduced quantities, where the length and energy scales are $\sigma_1$ (the HS diameter of the solvent species) and $kT$, respectively. For each calculation we must also select a thermodynamic state point, which we characterize by setting the solution composition and either the volume fraction, $\phi$, or the reduced pressure, $p^* = p\sigma_1^3/kT$. HS properties are usually presented at fixed $\phi$, but we will present some results at fixed $p^*$ since laboratory conditions are usually at fixed $T$ and $p$.

### A. Binary solution ($m_3 = 0$)

We begin our discussion by examining a binary HS solution composed of one solvent and one solute species. The calculations for a binary solution also serve to validate the numerical algorithm described above, since these BMCSL-based $B_{22}^{osm}$ values are known analytically; our numerically calculated $B_{22}^{osm}$ match Simonin's analytic result[47] within the numerical tolerance. Figure 1 contains $(B_{22}^{osm} - A_{2,app})/B_{22}^{hs}$ as a function of $\sigma_2/\sigma_1$, the solute-to-solvent size ratio, at volume fractions of $\phi = 0.1, 0.2, 0.3$, and $0.4$. Since the solution is taken in the infinitely dilute limit of solute HS, these values of $\phi$ correspond to fixed pressures of $p^* = 0.291, 0.919,$ $2.28$, and $5.29$, respectively. The difference between $B_{22}^{osm}$ and $A_{2,app}$ is given relative to $B_{22}^{hs} = 2\pi\sigma_2^3/3$ (the pressure second virial coefficient of the HS solute[39]), which is typically
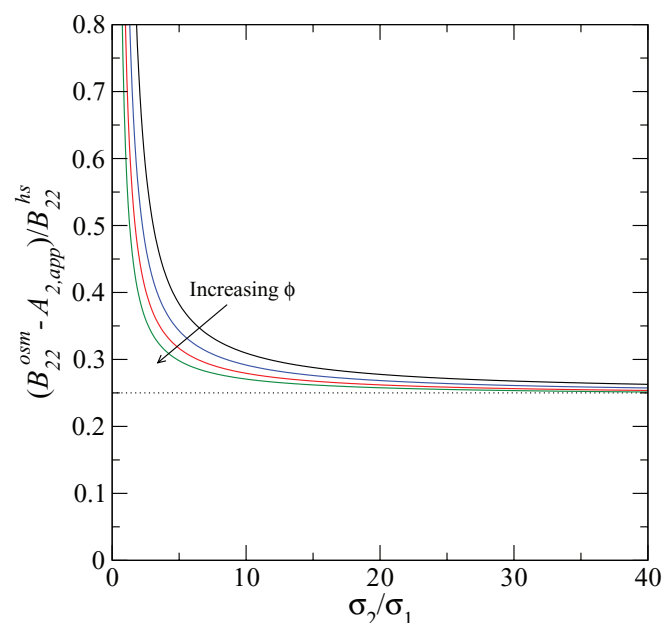
done when presenting an OSVC for proteins. The results in Fig. 1 indicate that $A_{2,app}$ is uniformly lower than $B_{22}^{osm}$ and that the difference between the two OSVCs relative to $B_{22}^{hs}$ decreases continuously as a function of $\sigma_2/\sigma_1$, approaching a nearly constant value that is only weakly dependent on $\phi$ at large $\sigma_2/\sigma_1$. The rate of decrease increases with volume fraction. At $\sigma_2/\sigma_1 = 40$, $(B_{22}^{osm} - A_{2,app})/B_{22}^{hs}$ falls between 0.25 and 0.26 for the $\phi$ in Fig. 1, with the largest difference found at lowest density. In Sec. V, we demonstrate that this difference is nearly constant and approximately equal to 0.25 in the limit of infinite size ratio.

### B. Ternary solution

We now examine ternary solutions of hard spheres, analogous to a solution containing solvent, protein solute, and a single cosolvent. In contrast to the calculations of $B_{22}^{osm}$ for a binary HS solution, OSVCs for ternary or higher HS solutions have not been previously presented. Inclusion of a third species adds two additional variables, the size ratio of cosolvent to solvent ($\sigma_3/\sigma_1$) and the molality of cosolvent ($m_3 = N_3/N_1$). The molality unit used here differs from the normal definition, moles of cosolvent per unit mass of solvent, to avoid introducing a molecular weight of the HS species. If the solvent HS is assumed to be water, conversion of our $m_3$ to the normal SI unit of molality (mol/kg $H_2O$) is accomplished by multiplying by $55.\bar{5}$.

Figure 2 contains $(B_{22}^{osm} - A_{2,app})/B_{22}^{hs}$ computed from the BMCSL EOS at $\phi = 0.2$ for $\sigma_2/\sigma_1 = 5, 10, 15,$ and $20$ as a function of cosolvent molality, where $\sigma_3/\sigma_1 = 2$. Since the composition of the solution is changing at fixed $\phi$, the pressure varies with $m_3$. For $\sigma_3/\sigma_1 = 2$, $p^*$ decreases monotonically from 0.918 to 0.187 as the molality increases



FIG. 1. Difference between $B_{22}^{osm}$ and $A_{2,app}$ relative to $B_{22}^{hs}$ plotted versus the protein-solvent size ratio, $\sigma_2/\sigma_1$, for volume fractions $\phi = 0.1$ (black), 0.2 (blue), 0.3 (red), and 0.4 (green). These fluid volume fractions correspond to reduced pressures of $p^* = 0.291, 0.919, 2.28,$ and $5.29$, respectively. The dotted line indicates the vertical position of 0.25.
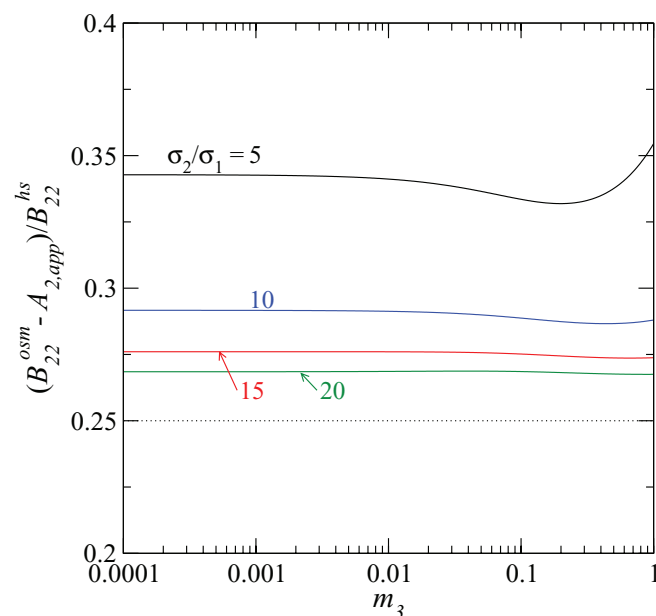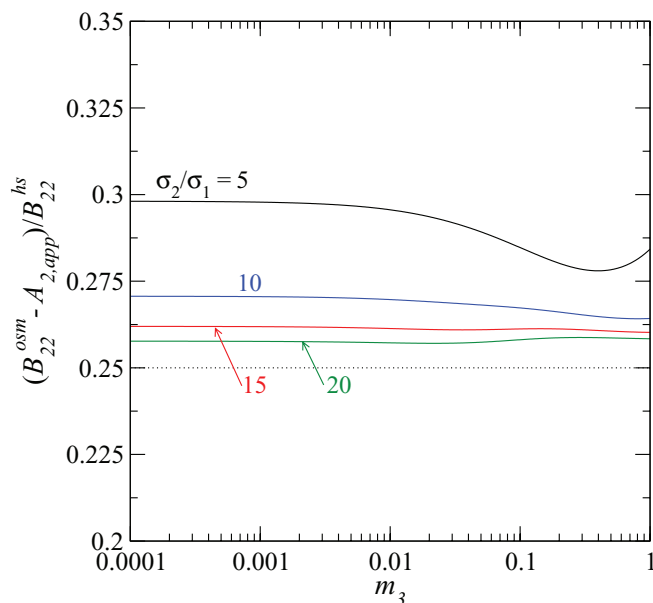


FIG. 2. Difference between $B_{22}^{osm}$ and $A_{2,app}$ relative to $B_{22}^{hs}$ plotted versus the cosolvent molality, $m_3$, for protein-solvent size ratios $\sigma_2/\sigma_1 = 5$ (black), 10 (blue), 15 (red), and 20 (green). The volume fraction is $\phi = 0.2$ and the cosolvent-solvent size ratio is $\sigma_3/\sigma_1 = 2$. Solution pressure varies with $m_3$, as noted in the text. The dotted line indicates the vertical position of 0.25.

FIG. 3. As Fig. 2, but for $\phi = 0.4$.



FIG. 4. As Fig. 2, but for fixed reduced pressure $p^* = 1.0$. $\phi$ varies with $m_3$, as noted in the text.

from $10^{-4}$ to unity. For all four protein size ratios shown, $(B_{22}^{osm} - A_{2,app})/B_{22}^{hs}$ is virtually unchanged over most of the $m_3$ domain but exhibits a local minimum at some $m_3 > 0.1$. (This feature is not visible in Fig. 2 for $\sigma_2/\sigma_1 = 15$ and 20.) In the limit of $m_3 \rightarrow 0$, the solution is simply the binary HS solution mentioned previously and the OSVCs recover the binary solution values for the specified $\sigma_2/\sigma_1$ and $\phi$. Indeed, at $m_3 = 10^{-4}$, the values of $(B_{22}^{osm} - A_{2,app})/B_{22}^{hs}$ are nearly identical to those in Fig. 1 for $\phi = 0.2$ and the specified $\sigma_2/\sigma_1$. For example, at $\sigma_2/\sigma_1 = 10$, $(B_{22}^{osm} - A_{2,app})/B_{22}^{hs} = 0.2917$ at $m_3 = 10^{-4}$ and the binary HS value for the same $\phi$ and $\sigma_2/\sigma_1$ is 0.2915. For $m_3 \rightarrow \infty$, where the solution is composed of only cosolvent and solute (e.g., a binary solution with size ratio $\sigma_2/\sigma_3$), a similar limit for $(B_{22}^{osm} - A_{2,app})/B_{22}^{hs}$ is available by exchanging $N_3$, $G_{33}$, and $G_{23}$ for $N_1$, $G_{11}$, and $G_{12}$, respectively, in Eq. (13). Beyond these basic features of $(B_{22}^{osm} - A_{2,app})/B_{22}^{hs}$, we find that the difference between the two OSVCs, relative to $B_{22}^{hs}$, for a specified $\sigma_2/\sigma_1$ is not strongly dependent on $m_3$. The average value of $(B_{22}^{osm} - A_{2,app})/B_{22}^{hs}$ is 0.34, 0.29, 0.28, and 0.27 for $\sigma_2/\sigma_1 = 5$, 10, 15, and 20, respectively, with maximum deviation of 0.015. These reported differences are similar in magnitude to those reported in Fig. 1. These results suggest that under certain conditions $(B_{22}^{osm} - A_{2,app})/B_{22}^{hs}$ approaches a constant value.

Figure 3 contains $B_{22}^{osm}/B_{22}^{hs}$ and $A_{2,app}/B_{22}^{hs}$ plotted versus $m_3$ at $\phi = 0.4$ and $\sigma_3/\sigma_1 = 2$ for the same protein-solvent size ratios in Fig. 2. For this volume fraction and range of cosolvent molality, the pressure, $p^*$, decreases monotonically from 5.29 at $m_3 = 10^{-4}$ to 1.01 at $m_3 = 1$. For all four size ratios, $(B_{22}^{osm} - A_{2,app})/B_{22}^{hs}$ again varies little for low $m_3$. A local extremum is visible for each $\sigma_2/\sigma_1$ at an $m_3 > 0.1$, but this extremum is a local maximum for $\sigma_2/\sigma_1 = 15$ and 20, whereas all size ratios showed a local minimum at $\phi = 0.2$. The average value of $(B_{22}^{osm} - A_{2,app})/B_{22}^{hs}$ is approximately 0.28, 0.27, 0.26, and 0.26 for $\sigma_2/\sigma_1 = 5$, 10, 15, and 20, respectively, which are similar in size to those for the ternary solutions at $\phi = 0.2$. As in Fig. 2, the variation in $(B_{22}^{osm}$
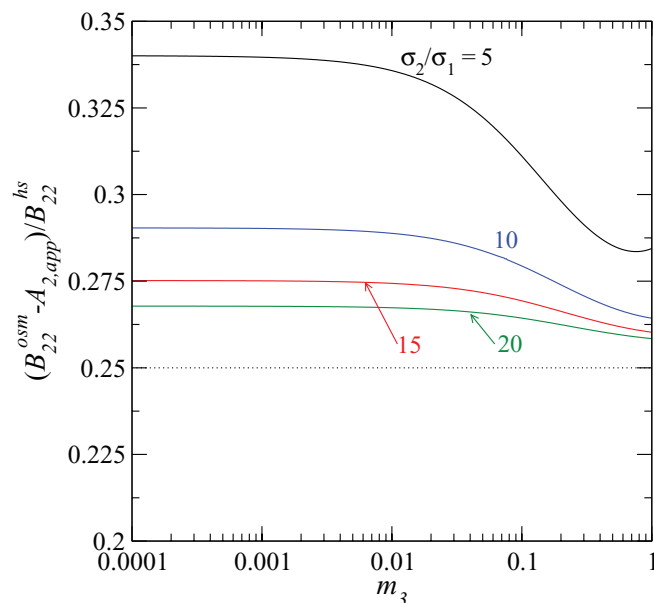
$- A_{2,app})/B_{22}^{hs}$ is small, with maximum deviation from the average of 0.015. It is again quite interesting to find consistency in the difference between $B_{22}^{osm}$ and $A_{2,app}$ for a variety of solution conditions.

Since the two previous figures plot data at fixed $\phi$, we include one data set at fixed pressure, for completeness. Figure 4 contains $(B_{22}^{osm} - A_{2,app})/B_{22}^{hs}$ plotted versus $m_3$ for $\sigma_3/\sigma_1 = 2$ at $p^* = 1$. For the molality range given, $\phi$ increases from 0.209 at $m_3 = 10^{-4}$ to 0.399 at $m_3 = 1$, which are thermodynamic state points that lie between those in Figs. 2 and 3. For all $m_3$, we again find that $(B_{22}^{osm} - A_{2,app})/B_{22}^{hs}$ is positive, indicating that $B_{22}^{osm}/B_{22}^{hs}$ exceeds $A_{2,app}/B_{22}^{hs}$, though the difference between those two OSVC ratios is not as narrowly bounded as it was at fixed $\phi$. For $\sigma_2/\sigma_1 = 5$, the difference between the OSVC ratios falls between 0.28 and 0.34, with the smallest difference at the largest $m_3$. For $\sigma_2/\sigma_1 = 10$, 15, and 20, the differences fall in the ranges 0.26–0.29, 0.26–0.28, 0.26–0.27, respectively, with the smallest differences again at the largest $m_3$. These are still, of course, small differences, but are indicative of the variation in $\phi$ while $m_3$ changes at fixed $p^*$.

All previous results were given for the single value of $\sigma_3/\sigma_1 = 2$, and so we now present some values of the OSVC ratios for different cosolvents. Table I contains $B_{22}^{osm}/B_{22}^{hs}$ and $A_{2,app}/B_{22}^{hs}$ for $\sigma_3/\sigma_1 = 1.5$, 3, and 6. If the solvent HS is taken to be "water" with radius 0.15 nm,[62] then these cosolvents have radii 0.225 nm, 0.45 nm, and 0.9 nm, which roughly correspond to the approximate spherical radii of urea (0.22 nm) (Ref. 62) and sucrose (0.43 nm) (Ref. 62) and the hydrodynamic radius of poly(ethylene glycol) (PEG) with a 1 kD approximate molecular weight (1 nm).[63] The cosolvent size ratios were thusly selected to at least approximate experimental solution conditions in terms of steric contributions. The protein hard spheres selected for the solution conditions in Table I are at $\sigma_2/\sigma_1 = 5$, 7.5, and 10, which correspond to sizes 0.75 nm, 1.125 nm, and 1.5 nm. These are not large pro-

TABLE I. Calculations of $B_{22}^{osm}/B_{22}^{hs}$ and $A_{2,app}/B_{22}^{hs}$ for three protein sizes ($\sigma_2/\sigma_1 = 5, 7.5,$ and 10) and three sample cosolvents ($\sigma_3/\sigma_1 = 1.5, 3,$ and 6) at the specified cosolvent molalities, all for the volume fraction of $\phi = 0.3$. The cosolvents sizes were selected to approximate urea, sucrose, and poly(ethylene glycol) with 1 kD molecular weight, dissolved in water, as described in the text.

| | | $\sigma_2/\sigma_1 = 5$ | | $\sigma_2/\sigma_1 = 7.5$ | | $\sigma_2/\sigma_1 = 10$ | |
| --- | --- | --- | --- | --- | --- | --- | --- |
| | | $B_{22}^{osm}/B_{22}^{hs}$ | $A_{2,app}/B_{22}^{hs}$ | $B_{22}^{osm}/B_{22}^{hs}$ | $A_{2,app}/B_{22}^{hs}$ | $B_{22}^{osm}/B_{22}^{hs}$ | $A_{2,app}/B_{22}^{hs}$ |
| | $m_3 = 10^{-3}$ | 0.564 | 0.248 | 0.811 | 0.520 | 1.588 | 1.309 |
| $\sigma_3/\sigma_1 = 1.5$ | $m_3 = 10^{-2}$ | 0.562 | 0.246 | 0.797 | 0.506 | 1.543 | 1.264 |
| (urea) | $m_3 = 10^{-1}$ | 0.553 | 0.239 | 0.708 | 0.417 | 1.248 | 0.969 |
| | $m_3 = 10^{-3}$ | 0.559 | 0.245 | 0.785 | 0.494 | 1.509 | 1.230 |
| $\sigma_3/\sigma_1 = 3$ | $m_3 = 10^{-2}$ | 0.537 | 0.235 | 0.639 | 0.355 | 1.037 | 0.761 |
| (sucrose) | $m_3 = 10^{-1}$ | 0.521 | 0.257 | 0.534 | 0.270 | 0.553 | 0.291 |
| | $m_3 = 10^{-3}$ | 0.497 | 0.229 | 0.593 | 0.327 | 0.953 | 0.692 |
| $\sigma_3/\sigma_1 = 6$ | $m_3 = 10^{-2}$ | 0.380 | 0.257 | 0.475 | 0.278 | 0.498 | 0.275 |
| (1 kD PEG) | $m_3 = 10^{-1}$ | 0.303 | 0.184 | 0.456 | 0.286 | 0.512 | 0.315 |

teins, of course, but the sizes were selected so that $B_{22}^{osm}/B_{22}^{hs}$ is the same or smaller order of magnitude as unity. (For large $\sigma_2/\sigma_1$, the BMCSL EOS yields $B_{22}^{osm} \gg 1$ (Ref. 47) that are not consistent with HS results that include depletion effects, which can lead to $B_{22}^{osm}/B_{22}^{hs} < 0$ (Refs. 49, 53, 64–67) depending on the balance of attractive and repulsive forces.[68–74]) In the table, the volume fraction is set to $\phi = 0.3$ and cosolvent molalities are $10^{-3}$, $10^{-2}$, and $10^{-1}$. [Recall that the molality may be converted to (mol/kg $H_2O$) by multiplying by $55.\bar{5}$.] For the majority of the cases shown, the relative difference between $B_{22}^{osm}/B_{22}^{hs}$ and $A_{2,app}/B_{22}^{hs}$ is similar to the results shown in Figs. 2 and 3, falling between 0.26 and 0.31. For the PEG cosolvent, however, the difference can be as low as 0.12 for the protein with $\sigma_2/\sigma_1 = 5$ and $m_3 = 10^{-1}$, rising only to 0.27 at the largest $\sigma_2/\sigma_1$ or lowest cosolvent molality. The particular results for the PEG cosolvent are not problematic, since the protein HS is similar in size to the cosolvent sphere for all three $\sigma_2/\sigma_1$ shown; for $\sigma_2/\sigma_1 \to \infty$, we still find that $B_{22}^{osm}/B_{22}^{hs}$ and $A_{2,app}/B_{22}^{hs}$ differ by 0.24–0.31.

## V. DISCUSSION

The interesting observation common to all data in the present report is that the difference between the BMCSL-derived $B_{22}^{osm}/B_{22}^{hs}$ and $A_{2,app}/B_{22}^{hs}$ is only weakly dependent on solution conditions when $\sigma_2/\sigma_1 \to \infty$ or, more practically, for both $\sigma_2/\sigma_1 \gg 1$ and $\sigma_2/\sigma_3 \gg 1$. The constant-$\phi$ results in Sec. IV indicate that for sufficiently large protein size, $B_{22}^{osm}$ and $A_{2,app}$ differ by $\alpha B_{22}^{hs}$, where $0.26 < \alpha < 0.31$, regardless of fluid volume fraction or cosolvent molality. Using some simple arguments, we can show that this relationship is well founded in the statistical mechanics of HS fluids.

To derive such an approximate relationship, we return to Eq. (13), which gives $A_{2,app}$ in terms of Kirkwood-Buff integrals. Using Eq. (8), we can substitute for $G_{22}$ to yield

$$\frac{A_{2,app}}{B_{22}^{hs}} = \frac{B_{22}^{osm}}{B_{22}^{hs}} + \lim_{N_2/V \to 0} \left[ \frac{G_{12}}{B_{22}^{hs}} - \frac{1}{2B_{22}^{hs}} \left( \frac{V}{N_1} + G_{11} \right) \right]. \quad (17)$$

Numerical inspection of results from the BMCSL EOS shows that for $\sigma_2/\sigma_1 \gg 1$, the term in parentheses including $G_{11}$ is

small compared to either $G_{12}$ or $B_{22}^{hs}$ and may be neglected for the purposes of this discussion. Thus, for $\sigma_2/\sigma_1 \gg 1$ we may approximate the difference between $B_{22}^{osm}$ and $A_{2,app}$ via:

$$\frac{B_{22}^{osm} - A_{2,app}}{B_{22}^{hs}} \approx - \lim_{N_2/V \to 0} \left[ \frac{G_{12}}{B_{22}^{hs}} \right]. \quad (18)$$

In a manner analogous to Eq. (8), $G_{12}$ may be written as[1]

$$G_{12} = \int_0^\infty \{\exp[-W_{12}(r)/kT] - 1\}4\pi r^2 dr$$
$$\approx -\frac{\pi(\sigma_1 + \sigma_2)^3}{6} + \cdots. \quad (19)$$

In the above equation, we have neglected all contributions to $G_{12}$ that do not result from the collision of protein and solvent hard spheres, i.e., the solvent-mediated interaction. Hence, for $\sigma_2/\sigma_1 \gg 1$,

$$\frac{B_{22}^{osm} - A_{2,app}}{B_{22}^{hs}} \approx \frac{\pi(\sigma_1 + \sigma_2)^3}{6} \cdot \frac{3}{2\pi\sigma_2^3} + \cdots$$
$$\approx \frac{1}{4}\left(1 + \frac{\sigma_1}{\sigma_2}\right)^3. \quad (20)$$

In the limit of $\sigma_2/\sigma_1 \to \infty$, the above relation approaches 1/4. Additionally, Eq. (20) indicates that $(B_{22}^{osm} - A_{2,app})/B_{22}^{hs}$ decreases towards its $\sigma_2/\sigma_1 \to \infty$ limit, which is visible in the bottom panel of Fig. 1. Numerical extension of the results in Fig. 1 to large $\sigma_2/\sigma_1$ confirms a limit similar to that in Eq. (20), where the deviations follow from terms neglected in Eqs. (17) and (19). Consequently, for solutions of hard spheres, $B_{22}^{osm}$ and $A_{2,app}$ differ by approximately $\alpha B_{22}^{hs}$ in the limit of $\sigma_2/\sigma_1 \to \infty$, where $\alpha \approx 0.25$. For solution conditions in which the net solvent contribution to $A_{2,app}$ (the neglected portions of Eqs. (17) and (19)) are on the same order of magnitude as $B_{22}^{hs}$, this argument must be adjusted. For hard spheres as modeled by the BMCSL equation, however, we find that this approximation is quite adequate. Finally, since $B_{22}^{osm}$ should be on the same order of magnitude as $B_{22}^{hs}$ and $(B_{22}^{osm} - A_{2,app})$ is approximately $0.25B_{22}^{hs}$, the difference between $B_{22}^{osm}$ and $A_{2,app}$ may be quantitatively significant compared to the actual value of $B_{22}^{osm}$. In experimental application,

however, the formal difference between $B_{22}^{osm}$ and $A_{2,app}$ may be obscured by the statistical uncertainty inherent to fits of Eqs. (1) and (2) to actual light scattering measurements.[34,42]

## VI. SUMMARY AND CONCLUSIONS

Following on work that discusses traditional and revised analyses of Rayleigh light scattering,[43] we have computed and compared two OSVCs for multicomponent solutions of hard spheres, $A_{2,app}$ and $B_{22}^{osm}$, that arise depending on how one treats the control volume in the analysis of light scattering data. The BMCSL-based results yield $B_{22}^{osm}$ and $A_{2,app}$ that differ only by a constant multiplied by $B_{22}^{hs}$ when the protein is much larger than the solvent and any cosolvent. That constant is approximately 0.25–0.30 for the HS solutions studied here and is only weakly dependent on solution conditions (cosolvent molality, cosolvent size, and either volume fraction or pressure). Examination of the mathematical form of $A_{2,app}$ suggests an approximate difference of $0.25B_{22}^{hs}$ between $B_{22}^{osm}$ and $A_{2,app}$ in the limit of infinite protein diameter. This result is not dependent on the selected BMCSL EOS, but was obtained directly from the statistical mechanical definitions of $B_{22}^{osm}$ and $A_{2,app}$.

The results given here suggest that $A_{2,app}$ and $B_{22}^{osm}$ for HS solutions differ in a systematic manner, and that the systematic difference between the two OSVCs is quantitatively nonnegligible. For HS solutions, this systematic difference is negative and $A_{2,app}$ is always smaller than $B_{22}^{osm}$. Whether these results directly translate to real protein solutions is unclear at present, since the HS contribution to the $G_{ij}$ integrals in real solutions may be obscured by long-range attractive or repulsive interactions. Regardless of the real molecular interactions, the mathematical definition of $A_{2,app}$ (Eq. (13)) may still yield a simple correlation between it and $B_{22}^{osm}$ if the solvent-solvent term ($G_{11} + 1/c_1$) is negligible and the solvent-protein term ($G_{12}$) is roughly constant or dominated by a HS-like contribution. We intend to evaluate this argument by adding attractive and/or repulsive perturbations to HS models of protein solutions, which may provide guidance concerning the relative values of $A_{2,app}$ and $B_{22}^{osm}$ for real fluids and further aid the interpretation of measurements in light scattering experiments.

## ACKNOWLEDGMENTS

[1]J. G. Kirkwood and F. P. Buff, J. Chem. Phys. **19**, 774 (1951).
[2]A. Ben-Naim, *Statistical Thermodynamics for Chemists and Biochemists* (Plenum, New York, 1992).
[3]B. L. Neal, D. Asthagiri, and A. M. Lenhoff, Biophys. J. **75**, 2469 (1998).
[4]J. R. Alford, B. S. Kendrick, J. F. Carpenter, and T. W. Randolph, Anal. Biochem. **377**, 128 (2008).
[5]T. L. Hill, J. Chem. Phys. **30**, 93 (1959).
[6]W. H. Stockmayer, J. Chem. Phys. **18**, 58 (1950).
[7]W. H. Stockmayer and H. E. Stanley, J. Chem. Phys. **18**, 153 (1950).
[8]S. N. Timasheff, H. M. Dintzis, J. G. Kirkwood, and B. D. Colemand, J. Am. Chem. Soc. **79**, 782 (1957).
[9]J. Narayanan and X. Y. Liu, Biophys. J. **84**, 523 (2003).
[10]P. R. Wills and D. J. Winzor, Prog. Colloid Polym. Sci. **119**, 113 (2002).
[11]R. J. Goldberg, J. Phys. Chem. **57**, 194 (1953).
[12]P. R. Wills, D. R. Hall, and D. J. Winzor, Biophys. Chem. **84**, 217 (2000).
[13]M. Deszczynski, S. E. Harding, and D. J. Winzor, Biophys. Chem. **120**, 106 (2006).
[14]D. J. Winzor, M. Deszczynski, S. E. Harding, and P. R. Wills, Biophys. Chem. **128**, 46 (2007).
[15]V. L. Vilker, C. K. Colton, and K. A. Smith, J. Colloid Interface Sci. **79**, 548 (1981).
[16]C. A. Haynes, K. Tamura, H. R. Korfer, H. W. Blanch, and J. M. Prausnitz, J. Phys. Chem. **96**, 905 (1992).
[17]L. W. Nichol, R. J. Siezen, and D. J. Winzor, Biophys. Chem. **9**, 47 (1978).
[18]H. V. Porschel and G. Damaschun, Stud. Biophys. **62**, 69 (1977).
[19]S. Y. Patro and T. M. Przybycien, Biotechnol. Bioeng. **52**, 193 (1996).
[20]V. Receveur, D. Durand, M. Desmadril, and P. Calmettes, FEBS Lett. **426**, 57 (1998).
[21]J. Behlke and O. Ristau, Biophys. Chem. **76**, 13 (1999).
[22]H. M. Schaink and J. A. M. Smit, Phys. Chem. Chem. Phys. **2**, 1537 (2000).
[23]P. M. Tessier, A. M. Lenhoff, and S. I. Sandler, Biophys. J. **82**, 1620 (2002).
[24]A. George and W. W. Wilson, Acta Crystallogr. **50**, 361 (1994).
[25]D. F. Rosenbaum and C. F. Zukoski, J. Cryst. Growth **169**, 752 (1996).
[26]B. L. Neal, D. Asthagiri, O. D. Veleve, A. M. Lenhoff, and E. W. Kaler, J. Cryst. Growth **196**, 377 (1999).
[27]P. M. Tessier and A. M. Lenhoff, Curr. Opin. Biotechnol. **14**, 512 (2003).
[28]A. C. Dumetz, A. M. Snellinger-O'Brien, E. W. Kaler, and A. M. Lenhoff, Protein Sci. **16**, 1867 (2007).
[29]B. Guo, S. Kao, H. McDonald, A. Asanov, L. L. Combs, and W. W. Wilson, J. Cryst. Growth **196**, 424 (1999).
[30]P. M. Tessier, V. J. Verruto, S. I. Sandler, and A. M. Lenhoff, Biotechnol. Bioeng. **87**, 303 (2004).
[31]J. Zhang and X. Y. Liu, J. Chem. Phys. **119**, 10972 (2003).
[32]W. F. Weiss IV, T. M. Young, and C. J. Roberts, J. Pharm. Sci. **98**, 1246 (2009).
[33]Y. Li, W. F. Weiss IV, and C. J. Roberts, J. Pharm. Sci. **98**, 3997 (2009).
[34]E. Sahin, A. O. Grillo, M. D. Perkins, and C. J. Roberts, J. Pharm. Sci. **99**, 4830 (2010).
[35]S. Ruppert, S. I. Sandler, and A. M. Lenhoff, Biotechnol. Prog. **17**, 182 (2001).
[36]E. Dickinson, M. G. Semenova, L. E. Belyakova, A. S. Antipova, M. M. Il'in, E. N. Tsapkina, and C. Ritzoulis, J. Colloid Interface Sci. **239**, 87 (2001).
[37]P. J. Loll, M. Allaman, and J. Wiencek, J. Cryst. Growth **232**, 432 (2001).
[38]P. C. Hiemenz and R. Rajagopalan, *Principles of Colloid and Surface Chemistry*, 3rd ed. (Marcel Dekker, New York, 1997).
[39]D. A. McQuarrie, *Statistical Mechanics* (University Science, Sausalito, 2000).
[40]N. Kern and D. Frenkel, J. Chem. Phys. **118**, 9882 (2003).
[41]A. C. Dumetz, A. M. Chockla, E. W. Kaler, and A. M. Lenhoff, BBA-Proteins Proteom. **1784**, 600 (2008).
[42]Y. Li, B. A. Ogunnaike, and C. J. Roberts, J. Pharm. Sci **99**, 645 (2010).
[43]M. A. Blanco, E. Sahin, Y. Li, and C. J. Roberts, J. Chem. Phys. **134**, 225103 (2011).
[44]D. Asthagiri, A. Paliwal, D. Abras, A. M. Lenhoff, and M. E. Paulaitis, Biophys. J. **88**, 3300 (2005).
[45]W. C. K. Poon and P. B. Warren, Europhys. Lett. **28**, 513 (1994).
[46]C. Vega, J. Chem. Phys. **108**, 3074 (1998).
[47]J.-P. Simonin, J. Phys. Chem. B **105**, 5262 (2001).
[48]D. Hall and A. P. Minton, Biochim. Biophys. Acta **1649**, 127 (2003).
[49]R. Roth, J. Phys.: Condens. Matter **17**, S3463 (2005).
[50]A. P. Minton, J. Pharm. Sci **96**, 3466 (2007).
[51]M. Jimenez, G. Rivas, and A. P. Minton, Biochemistry **46**, 8373 (2007).
[52]A. P. Minton, Biophys. J. **94**, L57 (2008).
[53]D. J. Ashton, N. J. Wilding, R. Roth, and R. Evans, Phys. Rev. E **84**, 061136 (2011).
[54]A. P. Minton, Biophys. J. **93**, 1321 (2007).
[55]T. Boublik, J. Chem. Phys. **53**, 471 (1970).
[56]N. F. Carnahan and K. E. Starling, J. Chem. Phys. **53**, 472 (1970).
[57]G. A. Mansoori, N. F. Carnahan, K. E. Starling, and T. W. Leland, Jr., J. Chem. Phys. **54**, 1523 (1971).
[58]W. G. McMillan and J. E. Mayer, J. Chem. Phys. **13**, 276 (1945).

[59] G. Scatchard, J. Am. Chem. Soc. **68**, 2315 (1946).
[60] J. G. Kirkwood and R. J. Goldberg, J. Chem. Phys. **18**, 54 (1950).
[61] N. F. Carnahan and K. E. Starling, J. Chem. Phys. **51**, 635 (1969).
[62] J. A. Schellman, Biophys. J. **85**, 108 (2003).
[63] Z. Luo and G. Zhang, J. Phys. Chem. B **113**, 12462 (2009).
[64] S. Asakura and F. Oosawa, J. Chem. Phys. **22**, 1255 (1954).
[65] A. Vrij, Pure Appl. Chem. **48**, 471 (1976).
[66] H. De Hek and A. Vrij, J. Colloid Interface Sci. **84**, 409 (1981).

[67] R. Roth, R. Evans, and A. A. Louis, Phys Rev. E **64**, 051202 (2001).
[68] R. Dickman, P. Attard, and V. Simonian, J. Chem. Phys. **107**, 205 (1997).
[69] B. Gotzelmann, R. Evans, and S. Dietrich, Phys. Rev. E **57**, 6785 (1998).
[70] J. R. Henderson, Physica A **313**, 321 (2002).
[71] D. W. Siderius and D. S. Corti, Phys. Rev. E **71**, 036142 (2005).
[72] D. W. Siderius and D. S. Corti, Phys. Rev. E **75**, 011108 (2007).
[73] A. R. Herring and J. R. Henderson, Phys. Rev. Lett. **97**, 148302 (2006).
[74] A. R. Herring and J. R. Henderson, Phys. Rev. E **75**, 011402 (2007).